SF2A 2018
P. Di Matteo, F. Billebaud, F. Herpin, N. Lagarde, J.-B. Marquette, A. Robin, O. Venot (eds)

SINGLE-MODE FIBER COUPLING FOR SATELLITE-TO-GROUND TELECOMMUNICATION LINKS CORRECTED BY ADAPTIVE OPTICS

C. B. Lim[1], C. Petit[1], K. Saab[1], B. Fleury[1], F. Mendez[1], J. Montri[1], N. Védrenne[1] and V. Michau[1]

Abstract. The need for high data rate communication systems has encouraged the development of new satellite-to-ground optical links using adaptive optics to compensate for atmospheric turbulence, while exploiting existing fiber components to limit their cost. Knowing the statistic distribution of the fading durations of the corrected flux coupled into a single-mode fiber is a cornerstone to design the optical transmission system (coding and interleaving protocols for example). Besides, results on such coupling efficiency statistics are not limited to the telecom applications and could be useful for astronomical applications, such as spectroscopy. In this context, an analytical model was developed at ONERA, along with a compact optical bench (LISA2), we integrated for experimental validation on the sky. Based on a previous study, an injection module was included to LISA2 to maximize the fiber-coupling and minimize the impact of static aberrations. The system integration along with the first results of its functional validation are presented.

Keywords: single-mode fiber, coupling, adaptive optics, telecommunication, satellite-to-ground

1 Introduction

Next generation satellite-to-ground laser communication systems have been identified as a promising alternative to radio frequency links to match the future need for very high data rate transmission links between space and the ground. Their implementation at a reasonable cost requires to exploit existing single-mode fiber (SMF) components already deployed for our ground telecommunication networks (amplifiers, multiplex transmitters). The signal emitted by the satellite laser terminal thus needs to be injected into a SMF after propagating in free space, which implies matching its intensity distribution and phase front with that of the fundamental mode of the SMF (Shaklan & Roddier 1988). However, atmospheric turbulence severely degrades the spatial coherence of the wave, which is critical for fiber coupling efficiency (CE), and results in power fluctuations, signal fades and eventually, propagation channel disruptions, with disastrous consequences for high data rates channels. Besides, in the particular case of low Earth orbit (LEO) satellites, scintillation, fast evolving turbulence, and strong operational constraints are to be expected. To limit these effects, mitigation techniques can be applied on the signal using interleaving or corrector error codes, or on the wavefront using adaptive optics (AO). Because they allow to compensate, in real time, the phase fluctuation induced by the atmospheric turbulence, AO systems are commonly used for ground-based observation applications and are becoming a key technology for free space optical communications. During the last decade, much effort was made to demonstrate AO systems dedicated to ground-space optical communication, with various in-lab achievements (Tyson et al. 2005; Berkefeld et al. 2010; Wilson & Roberts 2014). In 2015, NASA reported the first ground-based AO for optical downlink with the International Space Station using the Optical Payload for Lasercomm Science (Wright et al. 2015), including SMF coupling. In July 2015, Petit et al. (2016) demonstrated for the first time in Europe a LEO satellite-to-ground downlink with AO correction, the experiment was performed then with the SOTA terminal onboard SOCRATES microsatellite. In October 2015, AO demonstration for coherent detection was also presented by Tesat (Fischer et al. 2015). Furthermore, studies were dedicated to the assessment of using fiber coupling specifically for free space telecommunication (Poliak et al. 2016), but also SMF coupling at the output of large telescopes for spectroscopy or interferometry applications (Jovanovic et al. 2017). An analytical model describing the variations of the instantaneous coupled telecom flux into an SMF after partial

[1] ONERA/DOTA/HRA, F-92322 Châtillon, France

AO correction was also proposed (Canuet et al. 2018). Following these latest achievements, it appears necessary to further study the AO-corrected optical link performance limitations in terms of experimental SMF CE. In this paper, we report the integration and functional validation of a compact optical bench for LEO-to-ground telecommunication, with results in terms of AO correction and SMF coupling. In absence of a telecom signal from a satellite terminal, a preliminary experimental validation was performed on-star, and a second experiment planned in 2019 with a satellite telecom signal will complete this validation. The results are compared to that of a simplified simulation tool, presented in (Védrenne et al. 2012, 2014). In a first part, we describe the experimental setup and highlight the specificities of SMF injection. In a second part, the local atmospheric turbulence parameters are estimated. In a third part, we analyze the SMF coupling performance reached after AO-correction on the sky.

2 Experimental setup

The data presented in this study were acquired in June 2018 at the Observatoire de Côte d'Azur (OCA) using the Metrology and Optics (Meo) telescope and the LISA bench, which is an AO-assisted compact demonstrator for LEO-to-ground optical telecommunication link developped by ONERA using commercial on-the-shelf optical components. The first step of our work consisted in updating LISA to make it compatible with the use of SMF components. A SMF injection module was thus integrated with a twofold purpose: to estimate the SMF coupling performance in function of the turbulence conditions and to characterize the propagation channel. The obtained bench is called LISA2. The Meo telescope is located at an altitude of 1270 m, and its diameter is 1.5 m. It was selected due to its tracking and pointing performance adapted to LEO satellite-to-ground communication.

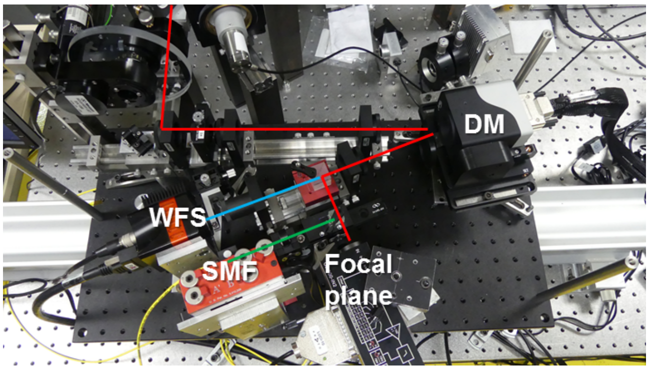

Fig. 1. LISA2 AO bench.

The LISA2 AO bench was designed and integrated by ONERA at the Coudé focus of Meo. Two stars were chosen: Arcturus (elevation 17°) and Antares (elevation 35°), due to their strong emission at 1.55 µm and to their elevations representative of that of a LEO satellite during closed loop measurement. Upstream from the enter of LISA2, a two-faces pyramid separated the light from the Coudé focus into two beams. Each beam had its own independant pupil of diameter 40 cm taken from the 1.5 m diameter telescope pupil. The first beam was dedicated to pupil imaging to allow pupil conjugation. The second beam was directed towards the LISA2 bench, which is illustrated by Fig. 1. The light enters LISA2 through a variable density wheel at the top left corner of the image and then undergoes beam reduction. The collimated beam reflects on the surface of a deformable mirror (DM), which realizes the bench pupil, and is then split and directed onto the wavefront sensor (WFS) (blue path) and the telecom path. In the telecom path, the beam is again split and directed into the SMF injection and detection module (green path) and onto the focal plane detector (red path) (which allows to measure scintillation and is used as a reference to estimate the SMF CE). Two InGaAs PIN detectors are used to measure the coupled signal at the ouput of the SMF (fibered detector) and the reference signal at the focal plane (300 µm diameter monodetector).

2.1 *Wavefront sensing and correction*

LISA2 uses a Shack-Hartmann wavefront sensor (SH-WFS) with 8x8 square subapertures, where the field of each subaperture covers 10x10 pixels in the focal plane. The WFS camera is a RAPTOR Owl camera (InGaAs

PIN-photodiode) with 320x256 pixels providing 0.8 quantum efficiency at 1.55 µm. Due to the very low intensity signal from the stars, slopes and intensities per subaperture were recorded with a frame rate of 500 Hz. The slope computation algorithm is a thresholded center of gravity (CoG). The threshold value is adjusted to limit background noise influence on the slope measurement. High order correction is performed by an ALPAO magnetic DM with 97 actuators, used in a 9x9 configuration for real-time correction. Based on its specification, it provides a ±5 µm mechanical stroke. From an in-lab calibration of the DM, the tensions command resulting in the mirror best flat surface was calculated and will be referred in the following as offset tensions. The AO loop is controlled by a Linux Personal Computer real-time controller (RTC) implementing various possible features both in terms of wavefront sensing and control algorithms. The sampling frequency was chosen accordingly to the WFS frame rate, as a result of the low intensity light available, 500 Hz. The overall loop delay was 2.2 frames due to RTC latency, with an effective rejection bandwidth of 30 Hz.

2.2 Single Mode Fiber injection

A SMF is designed to guide only the LP_{01} fundamental mode of the injected beam, which has a Gaussian intensity profile and a flat wavefront. The SMF coupling efficiency ρ_0 can be expressed as an overlap integral in the pupil plane of the SMF Gaussian mode and the injected wavefront Ruilier & Cassaing (2001) :
$\rho_0(\beta) = 2\left[\frac{1-exp(-\beta^2)}{\beta}\right]^2$,where $\beta = \frac{\pi}{2}\frac{D}{\lambda}\frac{\omega}{F}$, D being pupil diameter of the injected beam, λ the wavelength of operation, ω the radius of the LP_{01} mode at $1/e$ in the focal plane, and F the focal length of the transmission optic. ρ_0 has a theoretical maximum value equal to 82% (Shaklan & Roddier 1988) for $\frac{\omega}{F} = 0.71\frac{\lambda}{D}$, i.e. for $\beta = 1.115$. Assuming that the fiber be positionned in the image focal plane of the transmission optic, we have $\omega = \frac{\lambda F}{\pi\sigma}$, where σ is the radius of the SMF Gaussian mode LP_{01} at $1/e$ in the pupil plane. This leads to $D = 1.115 * 2\sigma$. The overlap integral (i.e. coupling efficiency) is sensitive to any deviation to this equality, as illustrated by Fig. 2 (top left figure).

The SMF injection was performed using a collimator illustrated in Fig. 2 (top right figure) of theoretical $1/e^2$ waist diameter 2.27 mm at the focal plane in front of the optic, and focal length F = 12.56 mm. Based on our optical design, the pupil diameter in front of the collimator was 2.4 mm. The optical alignment of this collimator is critical for SMF coupling optimization, as illustrated by Fig. 2 (bottom figures). Especially, the CE is strongly sensitive to any angular misalignment between the injected beam and the collimator optical axis: a 200 µrad tilt (which in our case is equivalent to about 1/3 of the diffraction angle $\frac{\lambda}{D}$) may result in a drop of the CE from the ideal value of 82% to 75%. As shown in the graph, in a non-ideal alignment state, the CE may drop from a value of for example 60% to 40%. This is why the alignment of the fibered collimator was performed using a 5-axis picomotor alignment stage allowing 3 translation directions and 2 rotations (rotation axis orthogonal to the direction of propagation) with < 30 nm and 1 µrad resolution.

3 Turbulence characterization

On the one hand, the Fried parameter r_0 was estimated using a generalized differential image motion monitor (GDIMM) located several dozen meters from the telescope (Aristidi et al. 2014). The source used for the measurement was the star Antares, which elevation was 35° at 23:00:00. The estimated seeing was 0.7 arcsec at zenith at 500 nm, which corresponds to very weak atmospheric perturbation (standard seeing values being around 1-2 arcsec). This leads to $r_0 = 28$ cm at 1.55 µm at a 35° elevation, without accounting for the bias induced by the dome effect (Petit et al. 2016). The speed of wind at ground level was 1.4 m/s. On the other hand, the wavefront was spatially sampled by the WFS. The local slope of the wavefront in front of each subaperture was estimated from the position of the focal spot as compared to that of a plane wavefront, using a thresholded CoG computation method as mentioned earlier. As a result, the estimated Fried parameter from WFS measurement is $r_0 = 26$ cm, which is in good agreement with the GDIMM estimation.

The C_n^2 profile distribution along the line of sight was assessed using the same method as detailed in Petit et al. (2016). This is illustrated by Figure 3 (top figure).

4 SMF coupling performance

The quantity of interest for high data rate laser link is the SMF coupling efficiency $CE = \frac{I_{SMF}}{I_{FP}}$, where we define I_{SMF} as the intensity measured at the output of the SMF, and I_{FP} as the intensity measured in the focal plane. If the maximum CE is theoretically 82%, the CE experimentally obtained never reached this

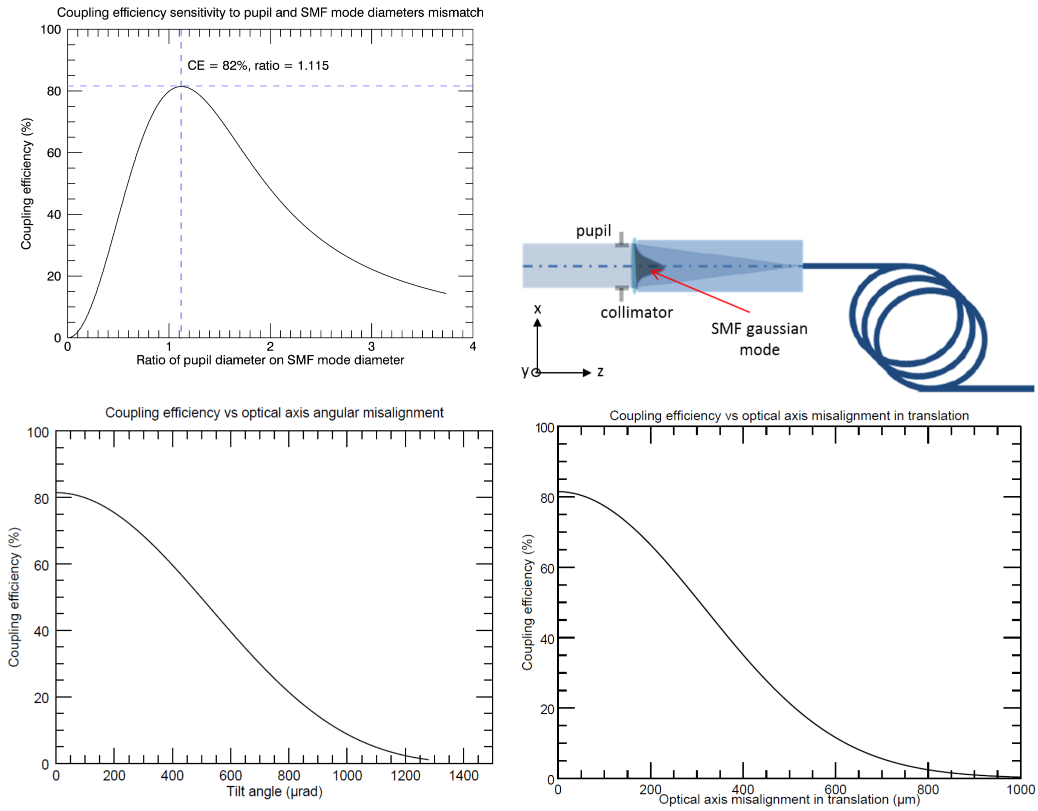

Fig. 2. Top left: Theoretical sensitivity of the CE versus pupil and SMF mode diameters ratio. **Top right:** Schematic of the SMF coupling of a collimated beam using a fibered collimator. **Bottom left:** Theoretical sensitivity of the CE versus injected wavefront and collimator optical axis angular misalignment (tilt). **Bottom right:** Theoretical sensitivity of the CE versus injected wavefront and collimator optical axis misalignment in translation (shift).

value. Identifying the transmission losses due to each optical component is necessary to correctly analyze the experimental performance in comparison to a realistic estimation of the maximum CE. This is why we developped a simple bench dedicated to establish a detailed error budget of the SMF coupling path, which is illustrated by Table 1. Similar to LISA2 perfectly aligned, a plane wavefront, provided by an internal source, is separated by a beam splitter into an SMF injection path and a focal plane detection path. The SMF injection path includes the fibered collimator, the 5-axis stage, the SMF. In Table 1, the first column ("Value") indicates the transmission rate of each optical component on the path. The second column displays the reliability of this value (i.e. 1-ϵ, ϵ being the error bar). The obtained CE value is the product of all values of the first column : 61.4%. Its reliability is the product of the terms of the second column : 76%. When accounting for this error bar, the maximum CE then drops to 46.7% in the most pessimistic case. As a reference, we used an internal collimated laser source at 1.55 μm and optimized the alignment of the fibered collimator to maximize the SMF CE with offset tensions applied to the DM. We obtained a maximum CE of 47%, which falls within our error budget.

For our experiment on the sky, the AO-loop was closed at a frequency of 500 Hz. Figure 3 (bottom left figure) shows the SMF CE vs time, measured on Antares at 35° elevation (the red solid line is the data smoothed by a moving average window). When switching from close to open AO loop, the mean CE drops from 27% to 5%. This minimum value may however be biased by the AO tip-tilt correction. In the configuration of an AO open loop with optimized SMF coupling, the mean CE was 11%. At low elevation (17°, Arcturus), the mean optimized CE was 24% in close loop and 11% in open loop.

These on-sky results at 35° must be compared to the internal performance which was of 47%. This deviation may stem from the combination of several effects. First, the large spectral band of the stars. The SMF intrinsequely performs a spectral filtering of the injected beam for the longer wavelengths, and the fibered collimator transmission bandwidth was a narrow window around 1.55 μm. On the contrary, no spectral filtering

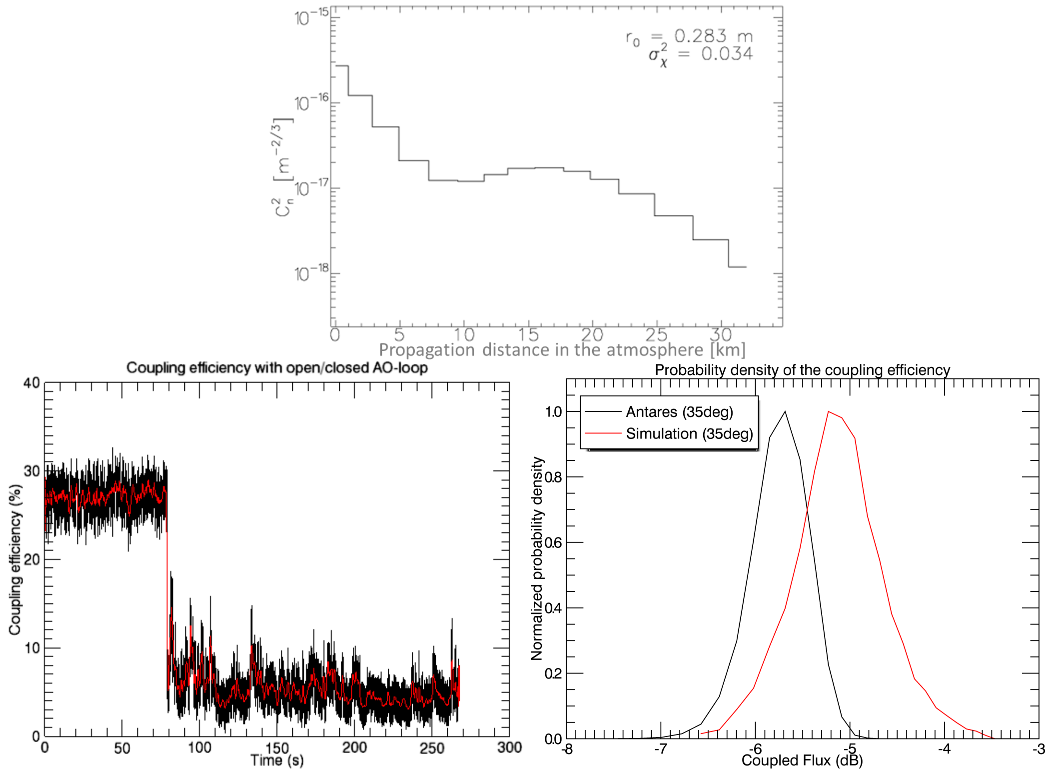

Fig. 3. Top: C_n^2 profile estimation obtained according to the same method as in Petit et al. (2016). **Bottom left:** SMF CE measured on Antares (35° elevation) and smoothed data in red, when switching from closed to open AO-loop. **Bottom right:** Probability density functions of CE for measurement and simulation.

	Value	Reliability
Scintillation	100%	97%
Exp. meas.	100%	99%
Pupil dimension	75%	93%
T_{collim}	98.9%	97%
Diff. aberr.	97.5%	98%
SR_{collim}	96%	98%
Fiber connector	97%	99%
Fiber Fresnel (in)	96%	99%
T_{fiber}	99.3%	99%
Fiber Fresnel (out)	96%	99%
Collim. alignment (x-axis)	100%	99%
Collim. alignment (y-axis)	100%	99%
Collim. alignment (azimuth)	100%	99%
Collim. alignment (elevation)	100%	99%
CE_{max}	61.4%	76%

Table 1. Error budget on SMF coupling of an internal laser source: the scintillation induced by the relative stability of the laser, the the uncertainty on the cubes transmission ("Exp. meas."), the pupil and fiber mode dimensions matching, the transmission of the collimator and of the optic fiber T_{collim} and T_{fiber}, the collimator Strehl ratio SR_{collim}, the differential aberrations (between the path of focal plane detection and the path of SMF injection), the optical alignment of the collimator.

was performed on the signal detected by the focal plane monodetector used as a reference to compute the experimental CE. Indeed, the stars being relatively weak sources, using a spectral filter to narrow the spectral

bandwidth of the injected beam would have resulted in a too weak signal to perform any AO correction nor any SMF coupling. Furthermore, an additional analysis only based on the star spectrum would not be accurate since the transmission spectra of the optics on the path from the telescope to the input of LISA2 were not estimated, so that the spectral content of the injected beam around 1.55 µm is not known. In combination with the aberrations introduced by the optics on the injection path but not on the focal plane detection path (aberrations of the collimator, focus error on the collimator/SMF connection), this results in an underestimation of the CE. Furthermore, in our case, the reachable CE is limited by the feedback signal used in the close-loop regime being the residual phase aberration measurement. The commands to be applied to the DM are calculated through minimization of this residual phase, i.e. through the maximization of the Strehl ratio, which is not necessarily connected to the CE optimization (Weyrauch et al. 2002).
As a comparison, simulations using our simplified model SAOST configured with a Hufnagel Valley-type C_n^2 profile with a ground layer adjusted to be of comparable r_0 were run and resulted in an expected close-loop best CE of 29%, which is consistent with our experimental results (27%). This is illustrated by Figure 3 (bottom right figure). Especially, the full width at half maximum (FWHM) of the simulated density is larger (0.93 dB) than that of the experimental one (0.69 dB). This can be understood by considering the limits of our simulation model. Our correction performance model neglects the effects of noise propagation in the WFS measurement. Usually weak in the case of an optical link with the laser terminal of a satellite (high flux configuration), they should be significant when using a star as a source considering the much lower light flux. The model also neglects the spectral bandwidth, which is very narrow in the case of a satellite telecommunication (around a few nm), whereas the Antares and Arcturus stars emission are wideband. Quantifying these effects is possible by considering the spectra of the stars and the spectral transmission of all the optics on the propagation path (but will not be done within the scope of this paper).

5 Conclusions

The functional validation of the AO-bench LISA2 was conducted on the sky in June 2018 at the Côte d'Azur Observatory. Real-time correction of a turbulent wavefront using AO along with SMF coupling of the corrected wavefront was demonstrated using two stars as sources, with elevation and peak wavelength representative of that of a satellite optical link. Although the available flux level did not allow to perform any spectral filtering, resulting in a degradation of the CE, the use of AO correction allowed to gain a factor > 2 in the CE compared to an open-loop configuration in both cases of LEO satellites elevations. For the high elevation case, the obtained CE and its density of probability were compared to a simplified performance model with consistent results. This study paves the way towards a demonstration with a telecommunication satellite terminal.

The authors acknowledge financial support from CNES, fruitful discussions with G. Artaud, technical support and fruitful discussions with E. Samain.

References

Aristidi, E., Fanteï-Caujolle, Y., Ziad, A., et al. 2014, Proc. SPIE, 9145, 91453G
Berkefeld, T., Soltau, D., Czichy, R., et al. 2010, Proc. SPIE, 77364, 77364C
Canuet, L., Védrenne, N., Conan, J.-M., et al. 2018, Journal of the Optical Society of America A, 35, 148
Fischer, E., Berkefeld, T., Feriencik, M., et al. 2015, IEEE, 1
Jovanovic, N., Schwab, C., Guyon, O., et al. 2017, Astronomy & Astrophysics, 604, A122
Petit, C., Védrenne, N., Velluet, M. T., et al. 2016, Optical Engineering, 55, 111611
Poliak, J., Giggenbach, D., Mata Calvo, R., & Bok, D. 2016, Proc. SPIE, 9739, 973913
Ruilier, C. & Cassaing, F. 2001, Journal of the Optical Society of America A, 18, 143
Shaklan, S. & Roddier, F. 1988, Applied Optics, 27, 2334
Tyson, R. K., Tharp, J. S., & Canning, D. E. 2005, Optical Engineering, 44, 096003
Védrenne, N., Velluet, M.-T., Samain, E., & Courde, C. 2014, Proc. ICSOS, 5
Védrenne, N., Velluet, M.-T., Sechaud, M., et al. 2012, Proc. ICSOS, 6
Weyrauch, T., Vorontsov, M. A., Gowens, J., & Bifano, T. G. 2002, Proc. SPIE, 4489, 177
Wilson, K. E. & Roberts, L. C. J. 2014, Proc. ICSOS, 5
Wright, M. W., Morris, J. F., Kovalik, J. M., et al. 2015, Optics Express, 23, 33705